



Effect of Maspin gene methylation induced by specific shRNA sequences on the proliferation of oral squamous cell carcinoma HN13 cells

Jingwen Wu^{1,2#}, Yi Liu^{1,2#}, Wenjing Wang^{1,2}, Haichao Wang^{1,2}, Hongyi Zhang^{1,2*}

¹Department of Stomatology, The First Affiliated Hospital of Yangtze University, Jingzhou 434000, Hubei Province, China

²Department of Stomatology, The First People's Hospital of Jingzhou, Jingzhou 434000, Hubei Province, China

#These authors contributed equally to this work as co-first author

ARTICLE INFO

Original paper

Article history:

Received: February 02, 2023

Accepted: April 26, 2023

Published: April 30, 2023

Keywords:

Specific shRNA sequences, oral squamous cell carcinoma, HN13 cells, maspin gene methylation

ABSTRACT

It was to investigate the mechanism of Maspin gene methylation induced by specific shRNA primer sequences in the proliferation of oral squamous cell carcinoma (OSCC) cells. Human OSCC HN13 cell line was selected as the study object, and the corresponding specific shRNA primer sequences were designed to construct Maspin-shRNA recombinant adenovirus using human Maspin nucleotide sequences as the target gene, and it was transfected into HN13 cells. The growth curve, Maspin expression level, migration and invasion ability, and proliferation activity of the transfected cells were analyzed. The results showed that the growth efficiency of transfected cells was significantly improved, and the OD value at 450 nm of cells in the specific sequence group (SSG) was greater than that of cells in the non-specific sequence group (nSSG). Maspin methylation was higher in the SSG than in the nSSG ($P < 0.05$). The number of cell migration and invasion in the SSG was higher than those in the nSSG ($P < 0.05$). The proliferation activity of cells in the SSG was higher than that of cells in the nSSG ($P < 0.05$). It showed that specific shRNA sequences induced Maspin gene methylation to inhibit Maspin expression, thereby participating in the migration and invasion motility of oral squamous carcinoma cells and improving proliferative activity.

Doi: <http://dx.doi.org/10.14715/cmb/2023.69.4.10>

Copyright: © 2023 by the C.M.B. Association. All rights reserved.

Introduction

In China, cancer is the most common malignant tumor in the oral and maxillofacial region, sarcoma is less common, and squamous cell carcinoma is the most common among carcinomas, generally accounting for more than 80%; followed by glandular epithelial carcinoma (mucoepidermoid carcinoma, adenocarcinoma, adenoid cystic carcinoma, malignant pleomorphic adenoma, acinar cell carcinoma, etc.) and undifferentiated carcinoma; basal cell carcinoma and lymphoepithelial carcinoma are less common, and the former occurs mostly in the facial skin. Squamous cell carcinoma of the oral and maxillofacial region (referred to as squamous cell carcinoma) occurs mostly in adults aged 40 to 60 years in China, more often in men than in women (1-3). The sites were the tongue, cheek, gingiva, palate, and maxillary sinus. In recent years, despite some recent advances in diagnostic and therapeutic techniques for oral cancer, the mortality rate of oral cancer has not changed significantly, and 40% of confirmed patients eventually die of the disease (4,5). To date, early detection and correct treatment are still the keys to the treatment of oral cancer. However, because some oral cancers can be asymptomatic and small in the early stage, it is difficult to be detected, and once detected, most of them have progressed to a later stage (6). Therefore, it is of great significance to increase attention to oral cancer and explore the pathogenesis of oral squamous cell carcinoma (OSCC). Current studies have shown that the occurrence of oral cancer involves

changes in the expression of numerous genes, leading to intracellular molecular metabolism disorders, abnormal signaling pathway conduction, changes in cell structure or physiological function, and other problems, ultimately causing abnormal cell proliferation and the formation of malignant tumors (7).

Gene methylation refers to the process by which cytosine (C) in CpG dinucleotide on DNA molecules selectively adds methyl groups to form 5'-methylcytosine under the action of enzymes (8,9). CpG dinucleotides are often located near the transcriptional regulatory region of genes, and their methylation can cause changes in chromatin structure, DNA conformation, and DNA stability, thereby regulating the transcription and expression of genes. Hypomethylation activates gene transcription, whereas hypermethylation prevents gene transcription leading to gene silencing (10-12). Aberrant gene methylation is one of the most common epigenetic changes in tumorigenesis, which is characterized by decreased global methylation levels in the genome (oncogenes) and abnormally increased local methylation levels in CpG islands (tumor suppressor genes) (13). Therefore, the pathogenesis of OSCC may be associated with aberrant gene methylation. RNA interference is a specific and selective process that disrupts target gene expression. Methods to mediate RNA interference effects include chemically synthesized double-stranded small interfering RNA (siRNA), vector-based short hairpin RNA (shRNA), etc (14,15). shRNA is an RNA molecule that can be cloned into an expression vector and express

* Corresponding author. Email: liancai606539804@163.com

double-stranded siRNA, including two short inverted repeats separated by a stem-loop sequence in the middle to form a hairpin structure, which is controlled by the polIII promoter. Relative to siRNA, shRNA is synthesized in the nucleus, further processed, and transported into the cytoplasm, and then enters RISC to exert activity, and has the advantages of high stability, long duration of action, and low off-target rate (16).

In summary, the human OSCC HN13 cell line was selected as the study object, and the corresponding specific shRNA primer sequences were designed to construct Maspin-shRNA recombinant adenovirus using the human Maspin nucleotide sequence as the target gene, and it was transfected into HN13 cells. The growth curve, Maspin expression level, migration and invasion ability, and proliferation activity of the transfected cells were analyzed to deeply understand the mechanism of Maspin gene methylation induced by specific shRNA primer sequences in the proliferation of OSCC cells.

Materials and Methods

Cell materials

As the study subject, the human OSCC HN13 cell line was purchased from China Tongpai (Shanghai) Biotechnology Co., Ltd.

Cell culture and passage

Culture procedures: (1) HN13 cell line was inoculated into DMEM/F-12 (Dulbecco's Modified Eagle Medium/Nutrient Mixture F-12) medium (Guangzhou Jet Bio-Filtration Co., Ltd., China) at a density of 1×10^6 cells/well and cultured in an incubator containing 5% CO₂ at 37°C. When the cells grew to about 80%, 1.5 mL trypsin (Sangon Biotech (Shanghai) Co., Ltd., China) was added for digestion and it was incubated in an incubator containing 5% CO₂ at 37°C. DMEM/F-12 culture medium was then put and it was passaged at a ratio of 1:3 once every 3 days to obtain cells growing in the logarithmic phase.

The construction method of recombinant adenovirus

The human Maspin nucleotide sequence (Nanjing GenScript Biotechnology Co., Ltd., China) was used as the target gene, and the corresponding specific shRNA primer sequence and a non-specific primer sequence were designed to link the expression vector plasmid pGeneSIL-1.1 (Wuhan BioRun Biotechnology Co., Ltd., China). Plasmid recombination was then performed using the UE plasmid mini preparation kit (Suzhou UE Landy Biotechnology Co., Ltd., China), and the next experiment could be performed after sequencing was qualified. Maspin-shRNA recombinant adenoviruses were obtained by transferring Maspin-shRNA expression cassettes to adenoviral expression vectors. They were packaged with human embryonic kidney cells 293.

Adenovirus transfection method

HN13 cells were inoculated into DMEM/F-12 medium, 1×10^6 cells per well, and cultured at 37°C in 5% CO₂ incubator, with SSG and nSSG set. At the end of the culture, the cells were transferred to a medium having Maspin-shRNA recombinant adenovirus or empty adenovirus for 1 day, Maspin-shRNA recombinant adenovirus was added to the SSG, and empty adenovirus to the nSSG. The cells

were then transferred to DMEM/F-12 complete medium, and the growth of the cells was observed adopting a high-definition microscope, the growth curve was drawn, and the transfection efficiency was calculated.

RT-PCR experiment

When the cells grew to about 85%, total RNA was extracted adopting Trizol total RNA extraction kit (Shanghai Share-Bio Co., Ltd., China), cDNA was obtained using a reverse transcription kit (Shanghai Share-Bio Co., Ltd., China), and amplification to obtain target DNA. Glucose agar electrophoresis was then carried out to obtain the relative mRNA expression, and the degree of Maspin methylation in each group was calculated.

Immunoblotting experiment

When the cells grew to about 85%, RIPA lysis buffer I (Suzhou New Cell & Molecular Biotech Co., Ltd., China) was applied to extract the total protein of the cells. Sodium dodecyl sulfate-polyacrylamide gel electrophoresis was then carried out, obtaining protein bands of different molecular weights, and the protein bands were transferred to nitrocellulose membranes and blocked adopting skimmed milk powder blocking solution (1 x in TBST) (Shanghai LMAI Bioengineering Co., Ltd., China). Antibody culture can be performed 1 hour later. In addition to the primary antibody working solution, it was placed in a 4°C incubator for overnight culture, followed by adding a secondary antibody, and it was placed in a 37°C incubator for 1 hour. They were placed in a dark room for development, and relative Maspin expression was obtained by analysis applying ImageLab software.

Transwell migration assay

After the suspension of cells grown to approximately 85% in culture medium, 200 μL of cell suspension was added to the upper chamber of the Transwell and 600 μL of complete medium to the lower chamber of the Transwell, and it was incubated at 37°C in 5% CO₂ for 1 day. After culture, paraformaldehyde was put for fixation, with crystal violet to stain, and mounting, and four fields were counted with a high-definition microscope, obtaining the number of cell migrations.

Transwell invasion assay

The operating environment was maintained at 4°C, and Matrigel and associated equipment were pre-cooled, with Matrigel and fetal bovine serum-free medium mixed at 1:6, coated in the upper chamber, covering the entire chamber surface, and it was incubated at 37°C in 5% CO₂ for 1.5 hours. Matrigel that failed to successfully assemble was removed and it was hydrated. Following the suspension of cells grown to approximately 85% in culture medium, 200 μL of cell suspension was put in the upper chamber and 600 μL of complete medium to the lower chamber, incubating at 37°C in 5% CO₂ for 1 day. After the culture, the addition of paraformaldehyde for fixation, it was stained with crystal violet, mounted, and four fields were counted with a high-definition microscope for obtaining the number of cell invasions.

Cell proliferative activity

After 2 days of cell culture, cells were observed to be in the log phase and could be digested with trypsin, trans-

ferred to a centrifuge tube, centrifuged at 3,000 rpm for 20 minutes, and the supernatant was removed. Cells were resuspended with a complete medium to make single-cell suspensions. The cell suspension was put in 96-well plates at 100 μ L per well. CCK-8 solution was added at 1 day, 2 days, and 3 days of culture for 3 hours, and the OD value at 450 nm was detected applying a Thermo Scientific™ Varioskan™ LUX multifunctional microplate reader (Shanghai Yunyi Science and Technology Trading Co., Ltd., China).

Statistical methods

Data were analyzed applying SPSS 19.0 statistical software, mean \pm standard deviation ($\bar{x} \pm s$) to present measurement data, and percentage (%) to present enumeration data. Repeated measures analysis of variance was applied for comparisons between groups and two-way analysis of variance for comparisons within groups. Two-sided tests were statistically significant at $P < 0.05$.

Results

Cell growth curves

Figure 1 shows the cell growth curves of the two groups. The growth efficiency of transfected cells was clearly improved, and the OD value at 450 nm was clearly greater in the cells of the SSG versus the cells of the nSSG.

Comparison of Maspin methylation degree in cells

Figure 2 illustrates the degree of Maspin methylation in the two groups of cells. It was found that the Maspin methylation degree of cells in the SSG was $80.5 \pm 7.58\%$ and that in the nSSG was $12.5 \pm 3.42\%$. Maspin methylation

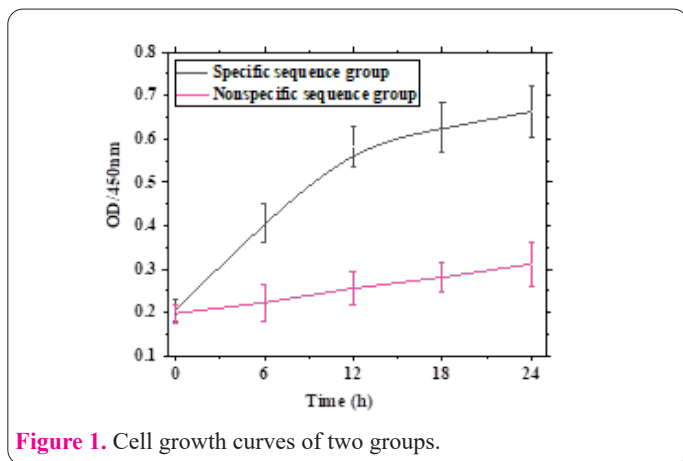


Figure 1. Cell growth curves of two groups.

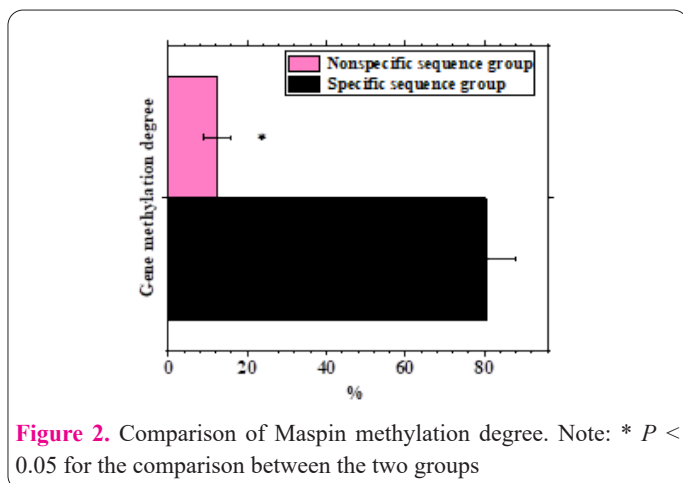


Figure 2. Comparison of Maspin methylation degree. Note: * $P < 0.05$ for the comparison between the two groups

was higher in cells in the SSG ($P < 0.05$).

Maspin mRNA expression level in cells

As illustrated in Figure 3, Maspin mRNA expression was 0.126 ± 0.021 in cells from the SSG and 0.155 ± 0.014 in cells from the nSSG. Maspin mRNA expression levels were lower in cells in the SSG ($P < 0.05$).

Maspin mRNA expression level in cells

As illustrated in Figure 3, Maspin mRNA expression was 0.126 ± 0.021 in cells from the SSG and 0.155 ± 0.014 in cells from the nSSG. Maspin mRNA expression levels were lower in cells in the SSG ($P < 0.05$).

Maspin protein expression level in cells

Figure 4 suggests the Maspin protein expression was 0.207 ± 0.038 in the cells of the SSG and 0.413 ± 0.055 in the cells of the nSSG. Maspin protein expression levels were lower in cells from the SSG ($P < 0.05$).

Cell migration and invasion

Figure 5 reveals the migration number of cells in the

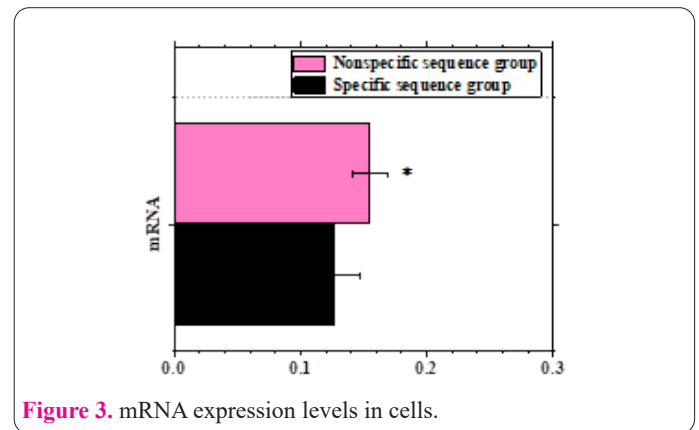


Figure 3. mRNA expression levels in cells.

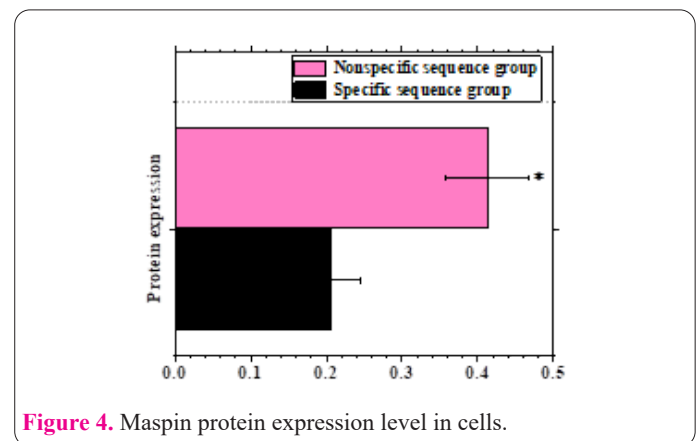


Figure 4. Maspin protein expression level in cells.

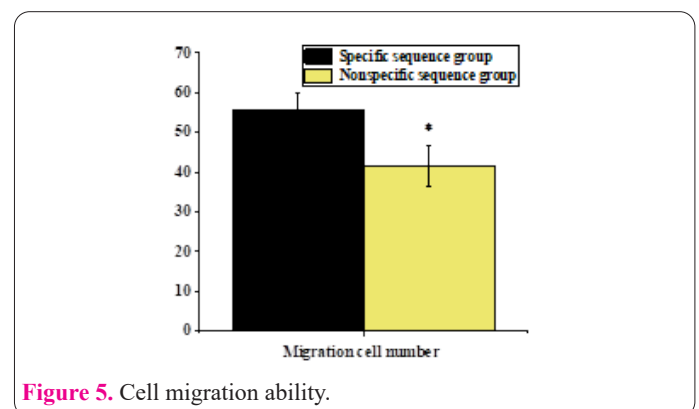


Figure 5. Cell migration ability.

SSG was 55.82 ± 4.21 , and that in the nSSG was 41.66 ± 5.07 . The number of cell migrations in the SSG was higher ($P < 0.05$). From the migration images, the cell migration effect of the SSG was obvious.

Figure 6 indicates the invasion number of cells in the SSG was 39.55 ± 4.08 , and that in the nSSG was 28.28 ± 3.15 . It revealed that the number of cell invasions in the SSG was higher ($P < 0.05$).

Comparison of cell proliferation activity

As illustrated in Figure 7, the proliferation activity of cells in the SSG was higher than that of cells in the nSSG ($P < 0.05$).

Discussion

OSCC, the most common malignant epithelial tumor of the head and neck region, is one of its main pathogeneses in which tumor cells can evade recognition and clearance by the body's immune system (17-19). The Maspin gene is located at 18q21.3, and the expression product has 375 amino acids, which is a tumor suppressor gene, and related studies have confirmed that the Maspin gene is able to induce tumor cell apoptosis from multiple pathways and hinder the migration and movement of tumor cells (20,21). Therefore, the human OSCC HN13 cell line was adopted as the study object, and the human Maspin nucleotide sequence was used as the target gene to design the corresponding specific shRNA primer sequence to construct Maspin-shRNA recombinant adenovirus, which was transfected into HN13 cells. First, from the growth curve, the growth efficiency of transfected cells was evidently improved, and the OD value at 450 nm of cells in the SSG was clearly greater in contrast with cells in the nSSG, which suggested that Maspin gene methylation induced by specific shRNA sequences could improve the growth efficiency of cells.

It has been clinically shown that methylation gene silencing of the Maspin gene is an important mechanism to promote the development and progression of the disease in the breast, thyroid, and digestive cancers (22,23). Maspin methylation was found to be higher in cells in the SSG ($P < 0.05$), suggesting that specific shRNA sequences induce successfully Maspin gene methylation, which becomes higher. Further analysis of Maspin expression indicated that Maspin mRNA and protein expression levels were lower in cells with specific sequences ($P < 0.05$), revealing that Maspin gene methylation induced by specific shRNA sequences would inhibit Maspin expression, and DNA methylation did effectively regulate Maspin gene. Cell migration refers to the characteristics of cells migrating from one place to another after stimulation by foreign signals, while cell invasion means the ability of cells to migrate from one area to another through the extracellular matrix or basement membrane matrix (24,25). It was found that the number of cell migration and invasion in the SSG was higher ($P < 0.05$), which indicated that Maspin gene methylation induced by the specific shRNA sequence could promote the migration and invasion of HN13 cells in vitro. In addition, the proliferation activity of cells in the SSG was higher ($P < 0.05$), and it was speculated that the specific shRNA sequence induced Maspin gene methylation to inhibit the expression of Maspin, thereby impro-

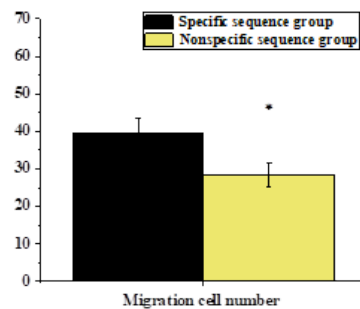


Figure 6. Cell invasion ability.

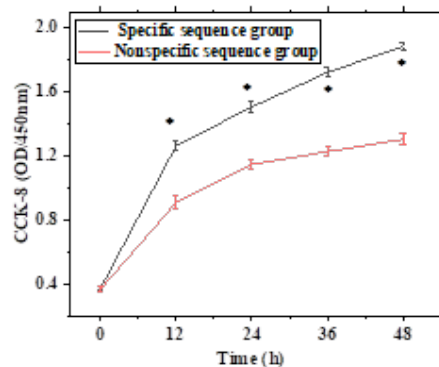


Figure 7. Comparison of cell proliferation activity.

ving the proliferation activity of oral squamous carcinoma cells.

A human OSCC HN13 cell line was applied to construct Maspin shRNA recombinant adenovirus by designing corresponding specific shRNA primer sequences with human Maspin nucleotide sequence as the target gene, and it was transfected into HN13 cells. The growth curve, Maspin expression level, migration and invasion ability, and proliferation activity of the transfected cells were analyzed. The results suggested that specific shRNA sequences induced Maspin gene methylation to inhibit Maspin expression, thereby participating in the migration and invasion of oral squamous carcinoma cells and improving proliferative activity. However, the grouping is relatively single, the cells are divided into SSG and nSSG, and the lack of comparative data of more sequences may have some impact on the results. In addition, there is a lack of in vivo experimental data and gene methylation will be considered for in vivo animal studies using experimental animals as study samples in later studies. In conclusion, this result provides a reference for the clinical diagnosis and treatment of OSCC.

References

- Guerrero ER, Claro AVO, Cepero MJL, Fernández JLA. Renal Failure Management in Patients with Metastatic Renal Cancer Receiving Nivolumab: Evaluation from Two Points of View. *Archivos Españoles de Urología* 2022; 75(9): 798-802 <https://doi.org/10.56434/j.arch.esp.urol.20227509.116>.
- Chen X, Shen Y, Ding B. Life-threatening bleeding after pelvic exenteration for recurrent cervical cancer: endovascular management of ruptured external iliac artery pseudoaneurysm: a case report and literature review. *Clin Exp Obstet Gynecol* 2022; 49(11): 252. <https://doi.org/10.31083/j.ceog4911252>.
- Lissoni A, Agliardi E, Peri A, Marchioni R, Abati S. Oral micro-

- biome and mucosal trauma as risk factors for oral cancer: beyond alcohol and tobacco. A literature review. *J Biol Regul Homeost Agents* 2020; 34(6(S3)): 11-17.
4. Wang AF, Li RG, Li R, Hongyan Qin HY. Clinical Efficacy of Anti-Tumor Decoction Combined With Chemotherapy in the Treatment of Advanced Oral Cancer and Its Effect on Serum Tumor Markers, T Lymphocyte Subsets and Survival Rates of Patients. *Acta Med Mediterr* 2021; 37: 2779. DOI: 10.19193/0393-6384_2021_5_428.
 5. Mirkeshavarz M, Ganjibakhsh M, Aminishakib P, Farzaneh P, Mahdavi N, Vakhshiteh F, Karimi A, Gohari NS, Kamali F, Khazafard MJ, Shahzadeh Fazeli SA, Nasimian A. Interleukin-6 secreted by oral cancer-associated fibroblast accelerated VEGF expression in tumor and stroma cells. *Cell Mol Biol* 2017; 63(10): 131–136. <https://doi.org/10.14715/cmb/2017.63.10.21>.
 6. Contaldo M, Lucchese A, Gentile E, Zulli C, Petruzzi M, Lauritano D, Amato MR, Esposito P, Riegler G, Serpico R. Evaluation of the intraepithelial papillary capillary loops in benign and malignant oral lesions by in vivo Virtual Chromoendoscopic Magnification: a preliminary study. *J Biol Regul Homeost Agents* 2017; 31(2(S1)): 11-22
 7. Johnson DE, Burtneß B, Leemans CR, Lui VWY, Bauman JE, Grandis JR. Head and neck squamous cell carcinoma. *Nat Rev Dis Primers* 2020 Nov 26; 6(1): 92. doi: 10.1038/s41572-020-00224-3. PMID: 33243986; PMCID: PMC7944998.
 8. Chamoli A, Gosavi AS, Shirwadkar UP, Wangdale KV, Behera SK, Kurrey NK, Kalia K, Mandoli A. Overview of oral cavity squamous cell carcinoma: Risk factors, mechanisms, and diagnostics. *Oral Oncol* 2021 Oct; 121: 105451. doi: 10.1016/j.oraloncology.2021.105451. Epub 2021 Jul 28. PMID: 34329869.
 9. Panarese I, Aquino G, Ronchi A, Longo F, Montella M, Cozzolino I, Rocuzzo G, Colella G, Caraglia M, Franco R. Oral and Oropharyngeal squamous cell carcinoma: prognostic and predictive parameters in the etiopathogenetic route. *Expert Rev Anticancer Ther* 2019 Feb; 19(2): 105-119. doi: 10.1080/14737140.2019.1561288. Epub 2019 Jan 15. PMID: 30582397.
 10. Yang Z, Yan G, Zheng L, Gu W, Liu F, Chen W, Cui X, Wang Y, Yang Y, Chen X, Fu Y, Xu X. YKT6, as a potential predictor of prognosis and immunotherapy response for oral squamous cell carcinoma, is related to cell invasion, metastasis, and CD8+ T cell infiltration. *Oncoimmunol* 2021 Jun 23; 10(1): 1938890. doi: 10.1080/2162402X.2021.1938890. PMID: 34221701; PMCID: PMC8224202.
 11. Vitória JG, Duarte-Andrade FF, Dos Santos Fontes Pereira T, Fonseca FP, Amorim LSD, Martins-Chaves RR, Gomes CC, Canuto GAB, Gomez RS. Metabolic landscape of oral squamous cell carcinoma. *Metabolomics* 2020 Sep 30; 16(10): 105. doi: 10.1007/s11306-020-01727-6. PMID: 33000429.
 12. Hasegawa K, Fujii S, Matsumoto S, Tajiri Y, Kikuchi A, Kiyoshima T. YAP signaling induces PIEZO1 to promote oral squamous cell carcinoma cell proliferation. *J Pathol* 2021 Jan; 253(1): 80-93. doi: 10.1002/path.5553. Epub 2020 Nov 5. PMID: 32985688.
 13. Dan H, Liu S, Liu J, Liu D, Yin F, Wei Z, Wang J, Zhou Y, Jiang L, Ji N, Zeng X, Li J, Chen Q. RACK1 promotes cancer progression by increasing the M2/M1 macrophage ratio via the NF- κ B pathway in oral squamous cell carcinoma. *Mol Oncol* 2020 Apr; 14(4): 795-807. doi: 10.1002/1878-0261.12644. Epub 2020 Feb 20. PMID: 31997535; PMCID: PMC7138402.
 14. McCord C, Kiss A, Magalhaes MA, Leong IT, Jorden T, Bradley G. Oral Squamous Cell Carcinoma Associated with Precursor Lesions. *Cancer Prev Res (Phila)* 2021 Sep; 14(9): 873-884. doi: 10.1158/1940-6207.CAPR-21-0047. Epub 2021 Jun 30. PMID: 34193432.
 15. Liu L, Wu Y, Li Q, Liang J, He Q, Zhao L, Chen J, Cheng M, Huang Z, Ren H, Chen J, Peng L, Gao F, Chen D, Wang A. METTL3 Promotes Tumorigenesis and Metastasis through BMI1 m6A Methylation in Oral Squamous Cell Carcinoma. *Mol Ther* 2020 Oct 7; 28(10): 2177-2190. doi: 10.1016/j.ymthe.2020.06.024. Epub 2020 Jun 24. PMID: 32621798; PMCID: PMC7544972.
 16. Flausino CS, Daniel FI, Modolo F. DNA methylation in oral squamous cell carcinoma: from its role in carcinogenesis to potential inhibitor drugs. *Crit Rev Oncol Hematol* 2021 Aug; 164: 103399. doi: 10.1016/j.critrevonc.2021.103399. Epub 2021 Jun 17. PMID: 34147646.
 17. Wang F, Liao Y, Zhang M, Zhu Y, Wang W, Cai H, Liang J, Song F, Hou C, Huang S, Zhang Y, Wang C, Hou J. N6-methyladenosine demethyltransferase FTO-mediated autophagy in malignant development of oral squamous cell carcinoma. *Oncogene* 2021 Jun; 40(22): 3885-3898. doi: 10.1038/s41388-021-01820-7. Epub 2021 May 10. PMID: 33972683.
 18. Rodrigues MFSD, Xavier FCA, Esteves CD, Nascimento RB, Nobile JS, Severino P, de Cicco R, Toporcov TN, Tajara EH, Nunes FD. Homeobox gene amplification and methylation in oral squamous cell carcinoma. *Arch Oral Biol* 2021 Sep; 129: 105195. doi: 10.1016/j.archoralbio.2021.105195. Epub 2021 Jun 8. PMID: 34126417.
 19. Wu P, Fang X, Liu Y, Tang Y, Wang W, Li X, Fan Y. N6-methyladenosine modification of circCUX1 confers radioresistance of hypopharyngeal squamous cell carcinoma through caspase1 pathway. *Cell Death Dis* 2021 Mar 19; 12(4): 298. doi: 10.1038/s41419-021-03558-2. PMID: 33741902; PMCID: PMC7979824.
 20. Ai Y, Liu S, Luo H, Wu S, Wei H, Tang Z, Li X, Lv X, Zou C. METTL3 Intensifies the Progress of Oral Squamous Cell Carcinoma via Modulating the m6A Amount of PRMT5 and PD-L1. *J Immunol Res* 2021 Aug 23; 2021: 6149558. doi: 10.1155/2021/6149558. PMID: 34476262; PMCID: PMC8408004.
 21. Ban Y, Tan P, Cai J, Li J, Hu M, Zhou Y, Mei Y, Tan Y, Li X, Zeng Z, Xiong W, Li G, Li X, Yi M, Xiang B. LNCAROD is stabilized by m6A methylation and promotes cancer progression via forming a ternary complex with HSPA1A and YBX1 in head and neck squamous cell carcinoma. *Mol Oncol* 2020 Jun; 14(6): 1282-1296. doi: 10.1002/1878-0261.12676. Epub 2020 Apr 13. PMID: 32216017; PMCID: PMC7266281.
 22. Puttipanyalears C, Arayataweegool A, Chalertpet K, Rattana-chayoto P, Mahattanasakul P, Tangjaturonsasme N, Kerekhan-janarong V, Mutirangura A, Kitkumthorn N. TRH site-specific methylation in oral and oropharyngeal squamous cell carcinoma. *BMC Cancer* 2018 Aug 6; 18(1): 786. doi: 10.1186/s12885-018-4706-x. PMID: 30081853; PMCID: PMC6080527.
 23. Srisuttee R, Arayataweegool A, Mahattanasakul P, Tangjaturonsasme N, Kerekhanjanarong V, Keelawat S, Mutirangura A, Kitkumthorn N. Evaluation of NID2 promoter methylation for screening of Oral squamous cell carcinoma. *BMC Cancer* 2020 Mar 14; 20(1): 218. doi: 10.1186/s12885-020-6692-z. PMID: 32171289; PMCID: PMC7071563.
 24. Li G, Jiang Y, Li G, Qiao Q. Comprehensive analysis of radiosensitivity in head and neck squamous cell carcinoma. *Radiother Oncol* 2021 Jun; 159: 126-135. doi: 10.1016/j.radonc.2021.03.017. Epub 2021 Mar 26. PMID: 33775714.
 25. Renzi A, Morandi L, Bellei E, Marconato L, Rigillo A, Aralla M, Lenzi J, Bettini G, Tinto D, Sabattini S. Validation of oral brushing as a non-invasive technique for the identification of feline oral squamous cell carcinoma by DNA methylation and TP53 mutation analysis. *Vet Comp Oncol* 2021 Sep; 19(3): 501-509. doi: 10.1111/vco.12688. Epub 2021 Mar 6. PMID: 33624422.